LLNL DARPA Mine Detection Field Experiment using RF

DCE-7

Scott D. Nelson
Defense Sciences Engineering Division,
Lawrence Livemore National Laboratory
7000 East Ave., L-153
Livermore, California 94550

Overview

Lawrence Livermore National Laboratory was involved in DARPA's mine detection field experiments at Ft. Carson, Colorado and Ft. A. P. Hill, Virginia during the fall of 1996 (October 14- 18, November 18-22). DARPA hosted a series of tests for the collection of clutter data using the latest technologies in the area of metallic and non-metallic mine detection techniques using electrical and/or magnetic sensing equipment. LLNL's role was to use high frequency radar to examine clutter areas and to examine the clutter environment in areas near intended targets.

The following information provides an introduction to the techniques that LLNL used, shows the equipment and data collection process, and presents some of the 3D volumetric reconstructions. The data is grouped by field site location but also flows from introductory material to complete reconstructions. The specific details about the data acquisition methodology, the data format, and the focused data sets are in the Appendices. Details about the radar unit itself are in the References.

Introduction

The data acquisition process, as outlined below, starts from raw time domain radar data from the radar system (bandwidth up to 7 GHz) and was then processed to allow for the radar, antenna, and surface effects. This involved using a micropower impulse radar to scan above the ground forming a 2D synthetic aperture. Presently, this scanning process is necessary since only one radar unit was used as part of the test; array configurations are being developed as part of other efforts which do not require this scanning. A physical array would simply drive along to sweep out an area.

The data was processed into 3D volumetric images after the field exercises were completed. The radar scanning system used in the experiments was a small, autonomous, and highly portable system for gentle terrain. The data acquisition effort at Ft. A. P. Hill used a more ruggedized version of the cart than was used at Ft. Carson but still only on gentle terrain.

This report is laid out in the format of two parallel and convergent topics: (1) the data acquisition process; and (2) the focused reconstruction imaging activities. Throughout this document, the two are intermixed and flow together in an attempt to paint a complete picture of the activities involved. As a consequence, some data from the first site is shown in the second section and vice versa. The imaging process that is outlined and the focused images that are presented are just meant to be representative of the process. The site-to-site detailed comparison is being handled by DARPA and their contractors as part of the comparison between the various target identification and characterization algorithms and is beyond the scope of this document.

Ft. Carson, Colorado

The Ft. Carson site consisted of two fields reserved for these mine detection activities by DARPA. Mines and unexploded ordnance were placed in known locations by the Waterways Experiment Station for DARPA. They also monitored the soil conditions during the testing. Efforts were made at the site to minimize the environmental effects during the data collection exercise. This allowed the emphasis of the exercise to be on the technologies involved and minimized the site evolution by all of the parties participating in the experiments.

Data Acquisition Process

The data acquisition process involved the use of a small scanning cart to support the radar unit, computer, and equipment. The system drives itself along as it takes data and uses a 2D scanning methodology due to the use of the single radar unit.

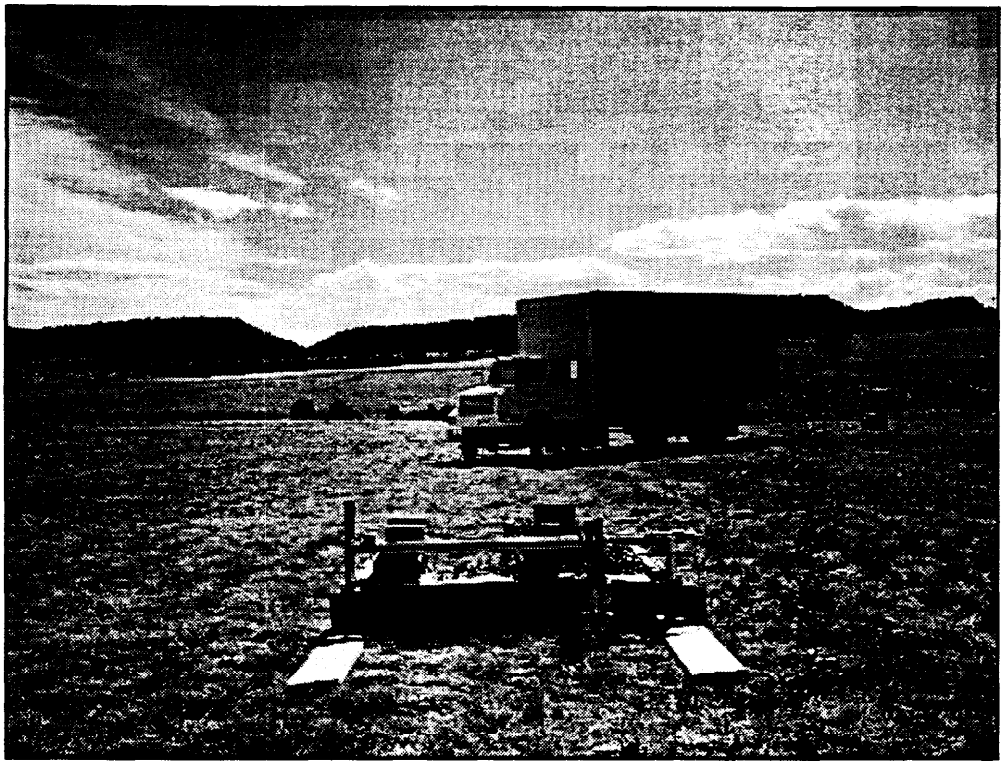

This photo shows the the LLNL radar cart at the Turkey Creek site as it scans across the ground using the radar. The boards shown in the foreground were for convenience.

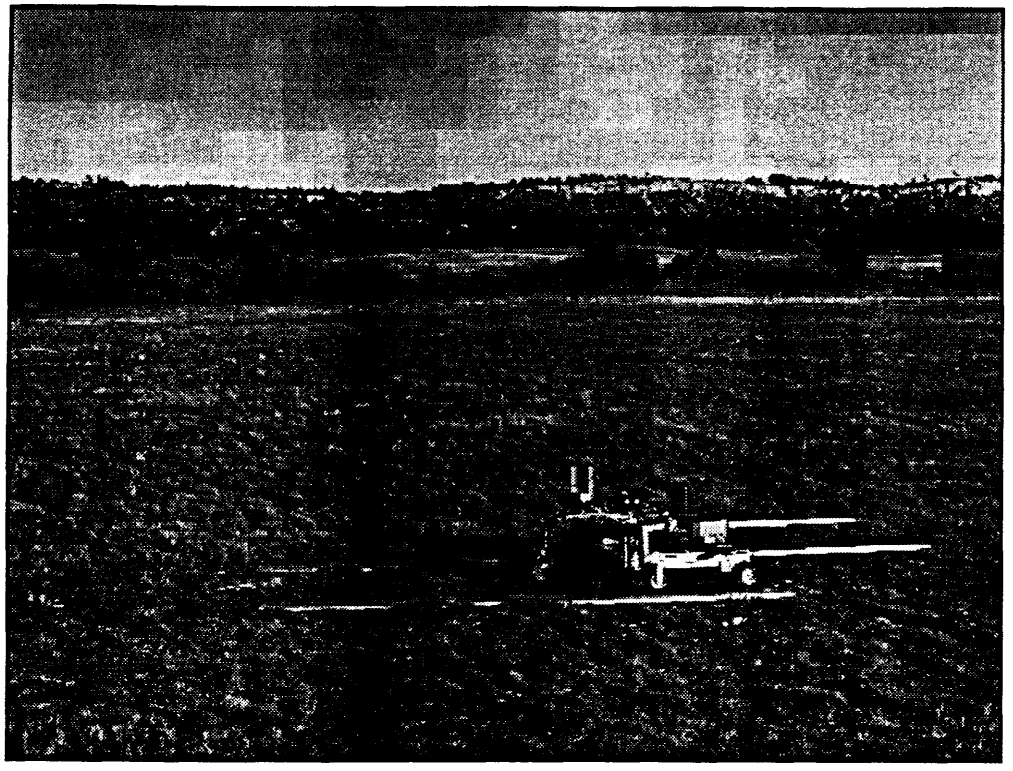

The Ft. Carson sites were selected because they presented a realistic, but best case, scenario. The local ground conditions were flat with occasional rolling hills and bumps. At the time of the LLNL testing, the sites were relatively free of ruts. It should be noted that the soil at these sites was firmer and probably had a higher clay content.

The transmit and receive modules were attached to the scanning arm and swept out a synthetic aperture across the ground. The transmit and receive radar units were encased inside the small insulating boxes shown in the photo to protect them from the 40°F temperature variation between the morning and the afternoon conditions.

The transmit and receive modules connected directly to their respective antennas. These antennas have an offset beam pattern (i.e. the peak in the main beam from the antennas is not along the physical axis of the antennas). The output from the receiver then went to the timing box and then to the computer's A/D converter.

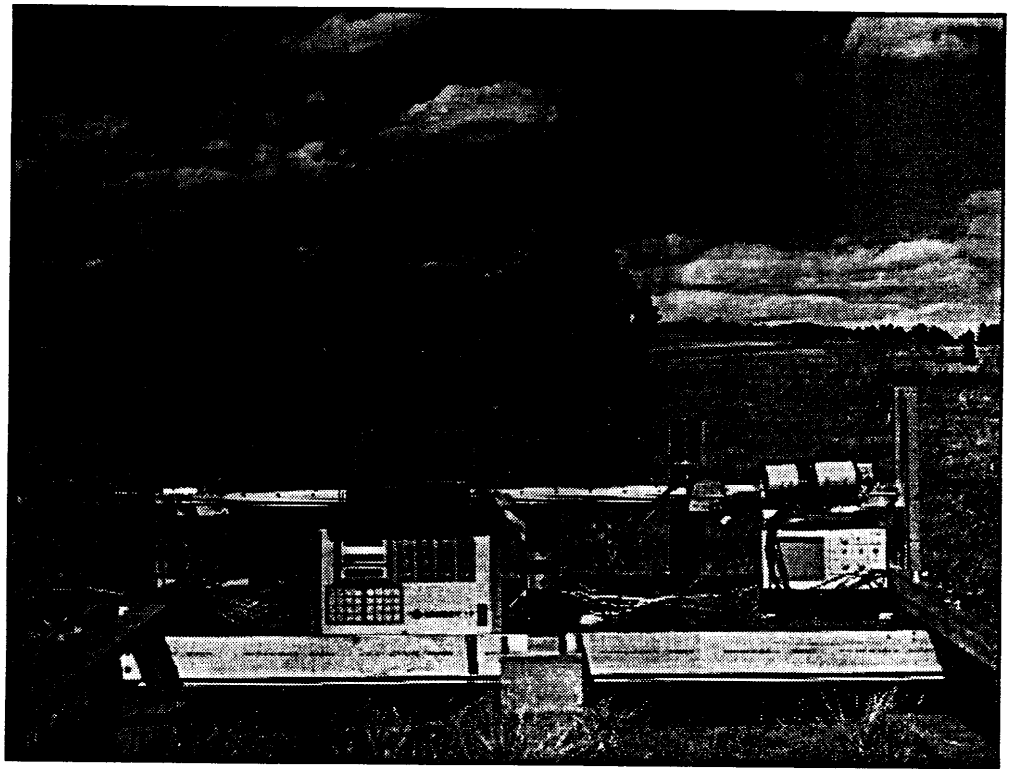

The cart moves the scanning arm left/right along the X axis and then moves the system forward 1 cm along the Y axis using the motor controller and computer. At each X,Y position, the radar acquired a time-domain waveform. The oscilloscope shown in the photograph was used to check the time-domain operational status at the start of a data session only. The small pink foam box on top of the oscilloscope houses the radar's timing box and was being thermally stabilized. This thermal instability caused a time drift in the data but the thermal stability problem was solved during the interim between the Ft. Carson and Ft. A. P. Hill testing. In either case, the time offset correction (see below) was used to realign the data.

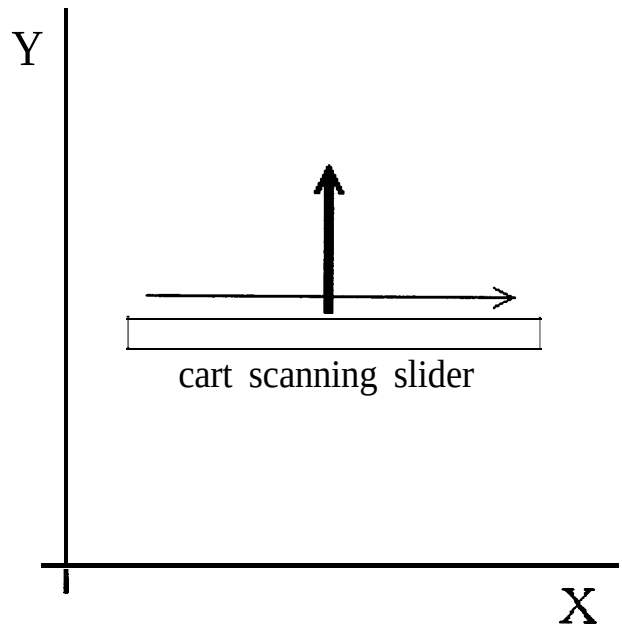

Data Processing

After the time domain radar data was stored on the computer's disk, it was then processed to remove the known effects in the data (radar pulse, antenna effects, etc.)

This is a view of a slice of the raw time domain radar data. This data has 1 cm spatial resolution using a synthetic aperture area scan. The horizontal axis is time and the vertical axis is the scan length along the transverse scan (the X axis).

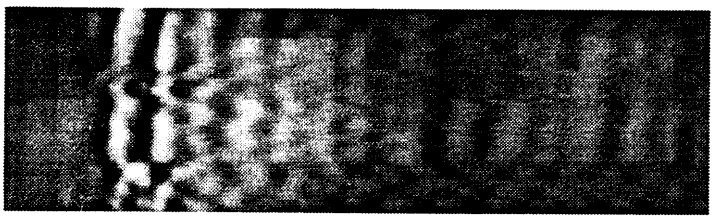

After source and antenna removal, the surface features of the soil are evident and dominate the data.

After surface compensation, the target scattering mechanisms are dominant. Note especially the two hyperbola easily visible in the raw time domain data. Each hyperbola was subsequently focused back to the original scattering bodies.

Preliminary results from the Ft. Carson site show the outline of the mine and the upper prongs. The flat surface of the upper part of the mine is visible as a bright radar return, the cylindrical side of the mine is seen as an elongated shape, and the prongs are seen up above the bright radar return.

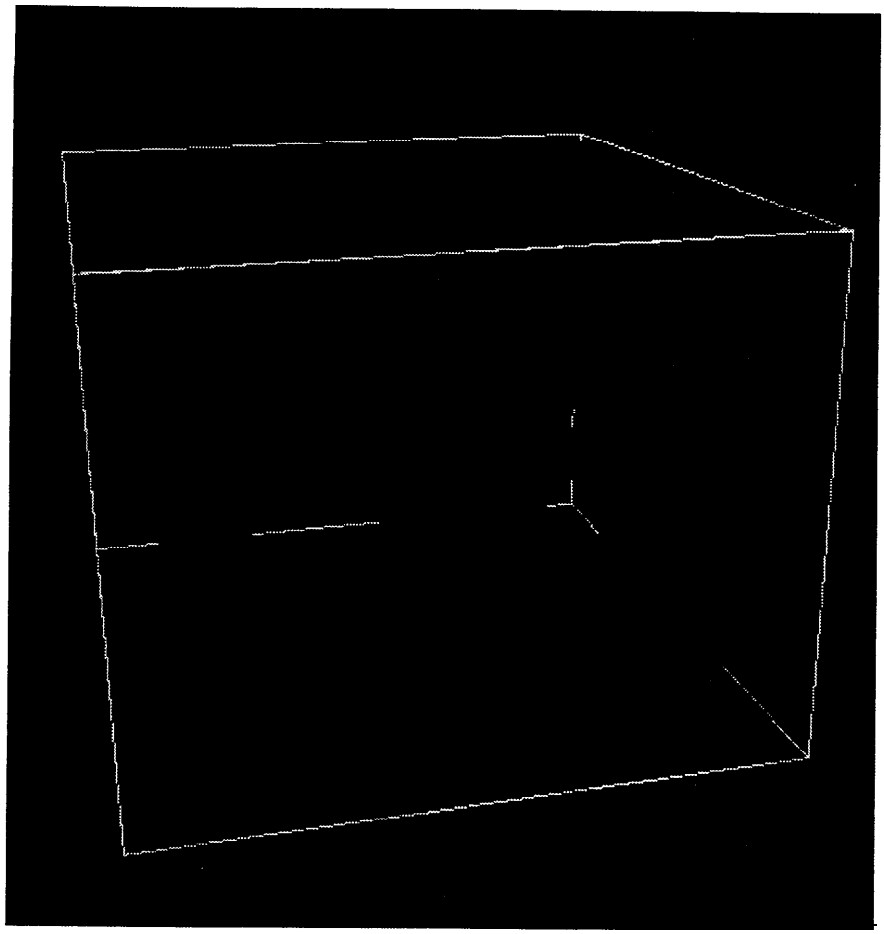

The filtered raw data is then focused using the electromagnetic focusing code [1] to generate the 3D volumetric image of Y9. A 2D perspective of the 3D volume is shown here. Note the main cylindrical body, the bright top surface reflection, and the prongs above that. The bounding box of the data set (1 m x 1 m x 0.3 m) is shown in yellow. The left-side face of the bounding box is not visible in this orientation.

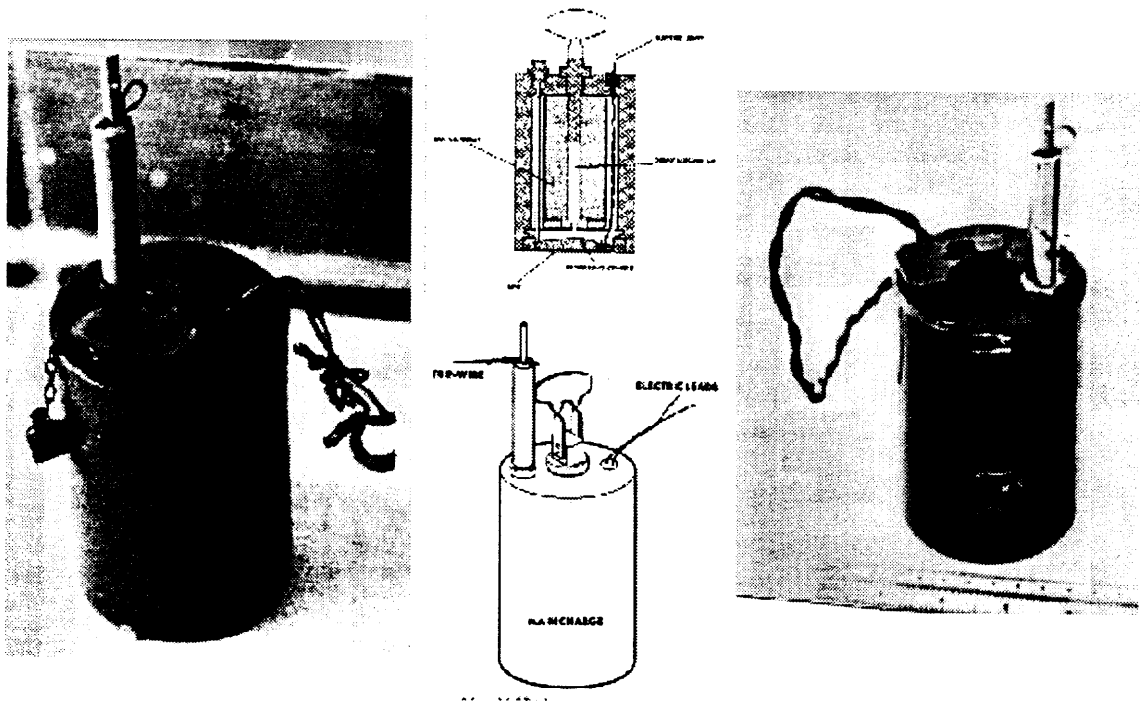

The above images show the OZM3 mine buried at point Y9 in each the test fields. Due to instrumentation of the thermisters near the mines, the exact configuration of the mines buried in the various fields is slightly different than that shown.

In addition to the targets that were buried by DARPA, there were also other features in the ground that LLNL was able to locate. The goal of the LLNL radar measurements was to characterize the local clutter environment in order to aid in the determination of object detection.

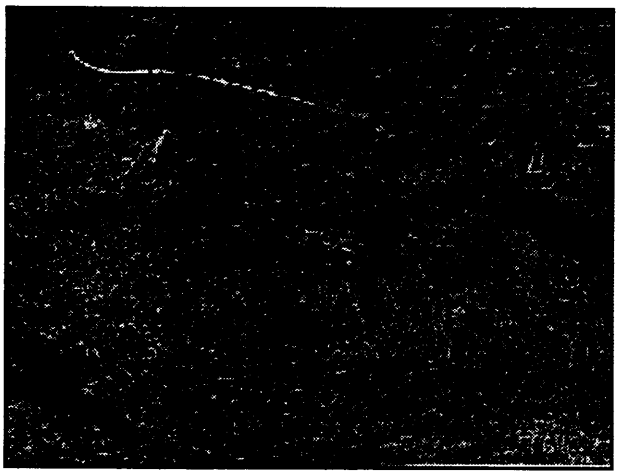

The shadow (right) is pointing to one of the many mouse tunnels (clutter sources) at both Ft. Carson sites. These tunnels constituted a network with several entrances and exits clearly visible from the surface.

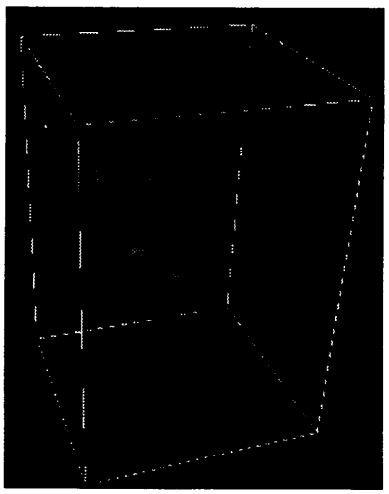

The mouse chambers and connecting tunnels are visible in this block of data extracted from the full 3D data set of Y21. Data threshold processing has been performed to make the features visible. Phase processing on the complete complex reconstructed data set would be able to determine which of the targets are holes (voids) and which are solid targets. No phase processing was performed on this data at this time.

Ft. A. P. Hill, Virginia

Arrival and setup

The Ft. A. P. Hill testing occurred approximately a month after the Ft. Carson testing. The basic configuration of the LLNL cart was the same as was previously used except that “off-road” tires were used instead of the previous tires that were designed for indoor use.

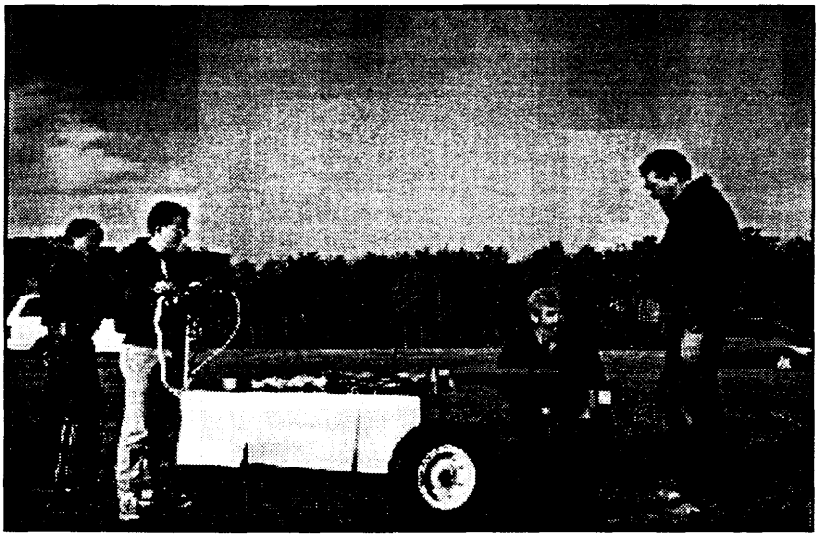

The scanning system, radar, and acquisition system remained unchanged although a higher gear ratio and drive system were used to compensate for the larger tires. A removable hard disk was also a recent addition to the system. The laptop computer, running Linux, acquired the data from the National Instruments A/D card and was stored on the hard disk. Unlike the previous testing at Ft. Carson, no attempt was made during this series of tests to connect the cart to the support trailer via the network cable since the cart could now operate using removable disk storage.

The landscape at Ft. A. P. Hill was similar to that at Ft. Carson but with less of a slope. The target placement of the mines in the fields used the same East-North layout as that used at the Ft. Carson sites [3].

Data acquisition

The synthetic aperture scanning method used at Ft. A. P. Hill was the same as that used at Ft. Carson. The cart scans transversely along the X axis, then moves forward 1 cm in the Y direction and repeats the X axis scan.

The radar scans left-right in front of the cart and acquires the synthetic aperture radar data. Unlike the Ft. Carson testing, the acquision system at Ft. A. P. Hill was bidirectional. The black microwave absorbing foam on the front of the cart was used to prevent interactions with the metal structure of the cart. Note that there were temporal reflections caused by the metal cords in the tires and the wheels. Microwave absorber was placed in front of these at an angle to reduce the reflections back into the receiver.

As part of the data acquisition and processing, it was necessary to perform two processing steps to compensate for the drift in the radar unit and data acquisition system (which is quite small in the Ft. A. P. Hill data) and to correct for the localized surface features.

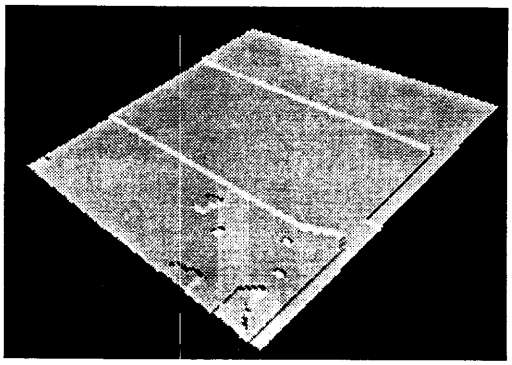

The time offset correction surface adjusts the time bias as a function of scan location. Since a typical acquisition cycle for a 1 m x 1 m area takes about 10 minutes using the synthetic aperture scanning technique, small perturbations in the time offset occur in the data. Note that these offsets are on the order of 40 ps (20 ps per “step” in the correction surface shown above) over a span of 10 minutes for the Ft. A. P. Hill data; and greater for the Ft. Carson data due to the previously mentioned thermal stability problem (fixed during the interim between Ft. Carson and Ft. A. P. Hill). The height axis in this model is the time drift; the other two dimensions are the X and Y spatial axes.

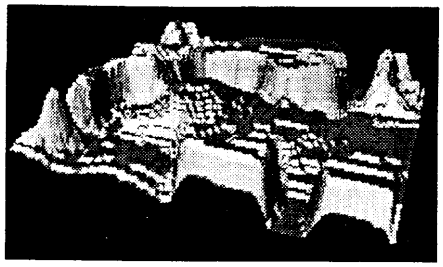

The ground topography correction surface aligns the reconstruction space of the data such that the high radar cross section (RCS) return from the ground can be reduced. The height axis in this model is time (which then maps to the spatial Z surface topography). The other two dimensions are the X and Y spatial axes.

Focused data

The data from the testing could be grouped into two categories: (1) regions of high target returns and (2) regions of high clutter returns. Other than the well defined calibration targets that are noted in the test plan [3], DARPA assigned a series of additional test points in the data sets.

Calibration targets

The following shows some of the highlights of the focused data from the four sites. No attempt has been made by LLNL to compare the site-to-site variance between the different sites when looking at the same target. That task is being handed out by DARPA to anyone requesting the data. These examples are presented here only to illustrate the kinds of data that are being generated.

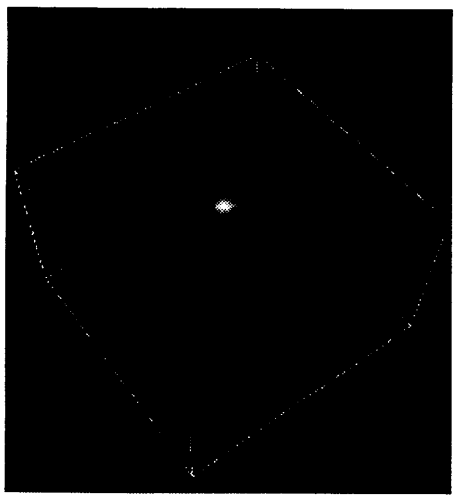

Test point Y2 (yellow 2) shows the outline of the teflon cylinder. No frequency dependent filtering has been performed on this data set.

After reconstruction, the focused data had a reconstruction cell size of 1 cm. This allowed for many voxels of resolution for the mine surrogates that were buried. The resolution cell size is a function of the frequency components used in the time domain waveform. For the ultra-wideband pulses generated by the radar, a 5 GHz instantaneous bandwidth allowed for a broad spectral coverage.

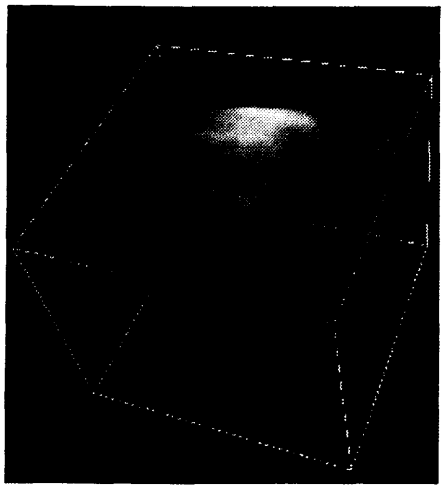

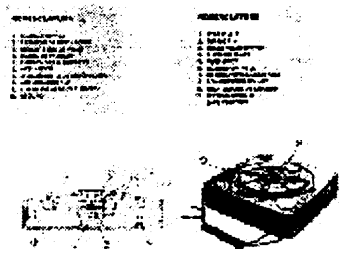

Test point Y7 (yellow 7) clearly shows the outline of the large rectangular Ml9 plastic anti-tank mine. No spatial filtering has been performed on this data. The rectangular outline is easily seen in this, and deeper, data slices.

Large dielectric objects, such as the teflon cylinder or the Ml9 antitank mine offer large RCS returns due to their dielectric mismatch with respect to the surrounding soil. The magnitude of the returns depends on the soil conditions, the dielectric, and the thickness of the dielectric.

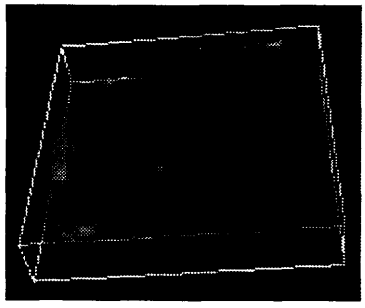

Several clutter sources (probably rocks) are clearly seen at the deeper depths in this thin slice of the Y8 (yellow 8) data set.

Additional test points

The objects in the remainder of the Yellow lanes were not identified but were selected by DARPA because they were “interesting.”

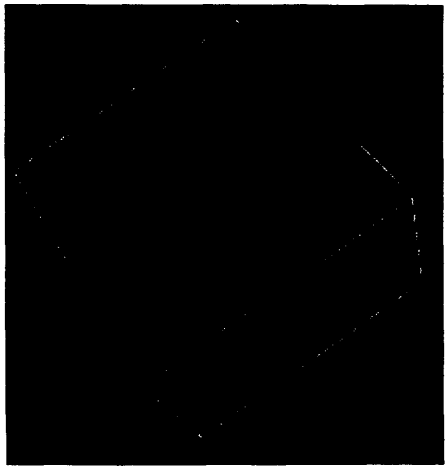

A small well-defined object is seen in Y 10 on the left side of the image.

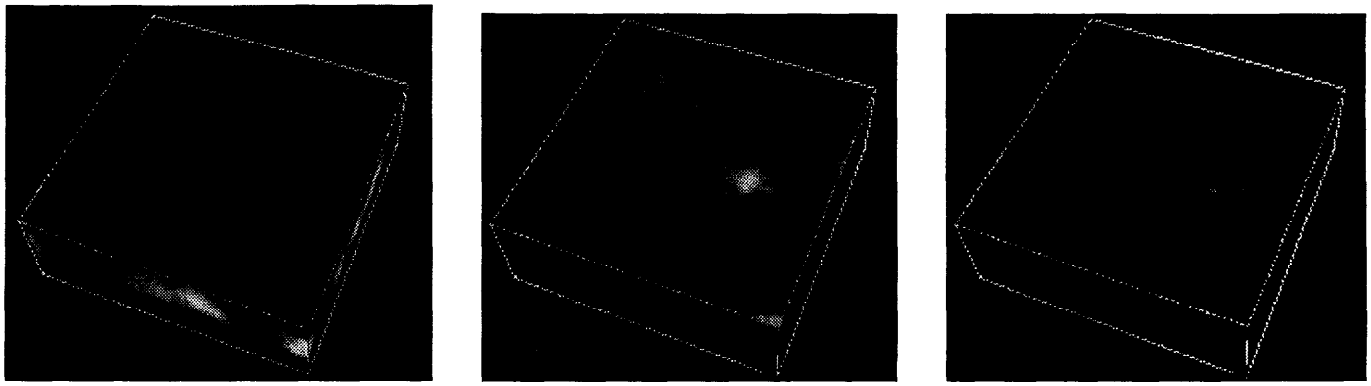

Circular objects display a series of “diffraction-like” rings due to the positive-negative nature of the time domain waveform. This makes them especially easy to see. Note the dark circle in the first slice, the bright spot in the second slice, and the dark circle in the third slice of Y 11.

Part of the utility of high resolution radar technologies is the ability to identify geometrical features of the objects. Boulders, tree roots, gopher holes, and strata would have non-regular geometries. Buried mines typically are cylindrical or rectangular solids. On the other hand, surface mines are designed to sit on the surface and blend in with the surroundings and come in a variety of shapes.

Environmental Conditions

Like Ft. Carson’s testing, the temperature variation at the Ft. A. P. Hill site was a source of problems in the radar unit and in the cart’s mechanical components. Steps had been taken in the interim between the Ft. Carson testing and the Ft. A. P. Hill testing to better stabilize the radar unit and the resulting performance was greatly improved over the previous testing. Unfortunately, the weather was not so kind to the team or the mechanical equipment.

Anne Andrews (second from left, representing DARPA) arrives on-site just in time for the snow storm. The team assembled a portable tent and placed microwave absorbing foam in front of the metal poles holding up the tent. The reflections in the time domain data caused by the upper supporting framework of the tent occurred later in the data set than the reflections from the targets of interest. As long as the snow remains a dry snow, then the effects of the snow on the data quality are small. Once the snow melts however, the ground becomes too reflective to resolve the clutter sources in the ground.

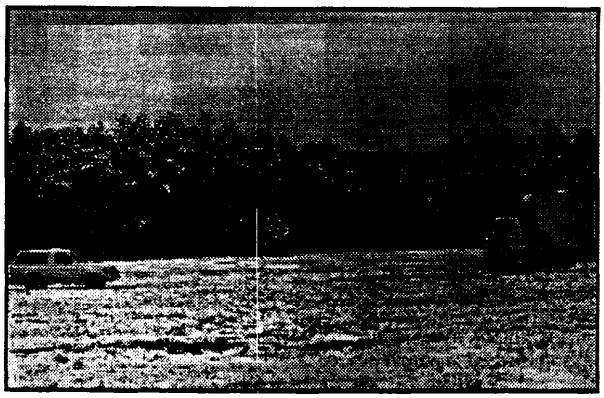

Although the data acquisition cart had no problems with the weather, the same could not be said for the support truck. Fortunately, the team was not reliant on the truck by this point.

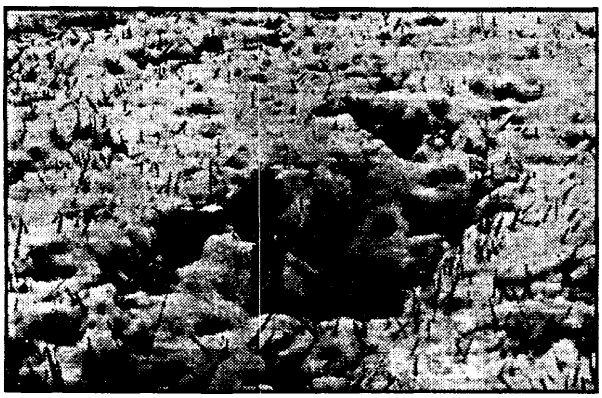

The ruts and local surface conditions were about 30 cm deep in some places in the field. The acquisition and focused reconstruction system was very sensitive to local surface contours and places such as this were avoided.

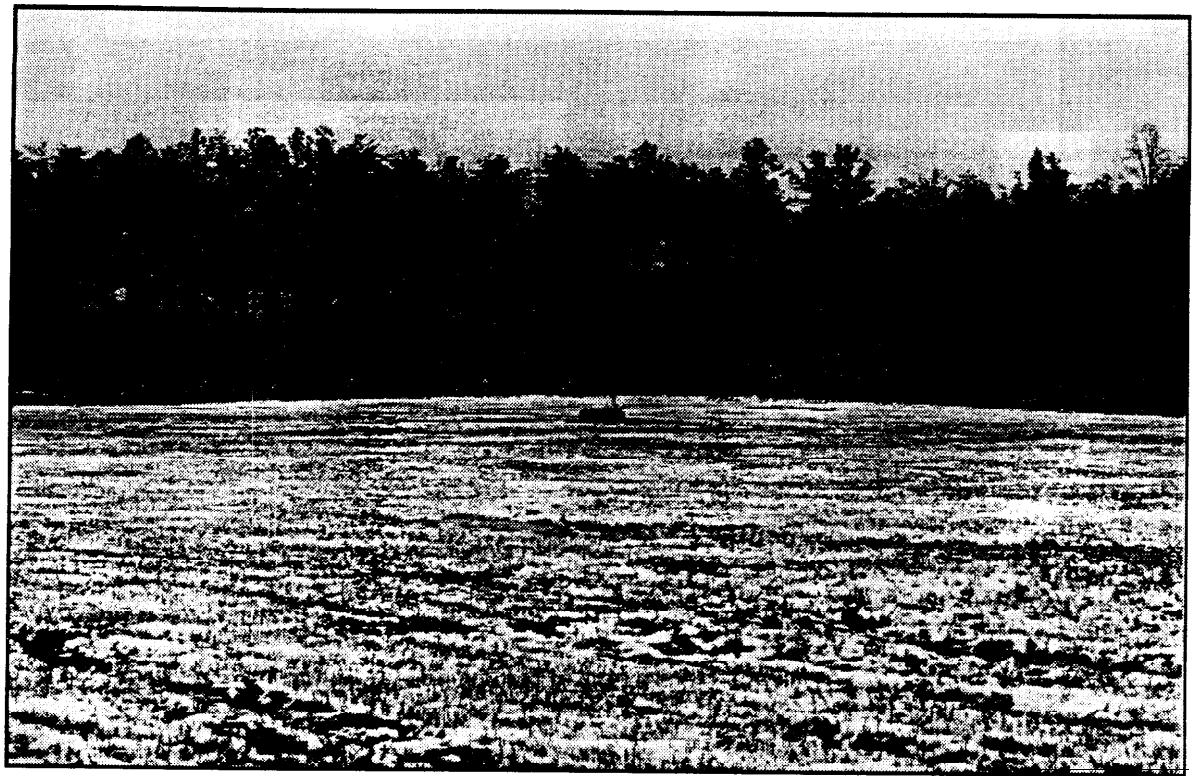

The cart autonomously acquires data using the on-board computer, disk storage, radar unit, motor controller, and UPS power supply (uninterruptible power supply). Initial testing used a small portable generator but it was discovered that it provided poor-quality power which resulted in bad data. That small generator was discarded and the cart was attached directly to a larger generator on the other side of the field (appx. 700 feet away). Future systems would use a larger UPS to remove the need for the on-going generator connection.

Conclusions

Initial experiences at the Ft. Carson site indicated a sensitivity to temperature extremes in the radar unit. These were corrected in the field using lights to stabilize the temperature and fixed permanently once the units returned to LLNL after completion of the first test series. These problems were caused by the use of off-the-shelf components in the interface box and did not involve the radar itself. These were easily identified and corrected in a temperature chamber.

Thus, the following can be concluded:

1. the mechanical system should be as simple as possible to avoid problems with environmental conditions
2. the radar unit should be well in front of the remainder of the cart structure to reduce RF interference from the structure
3. some small commercially available portable generators generate power of dubious quality which leads to unreliable operation/data
4. radar can detect plastic mines and metal mines, but holes (small animal tunnels) are difficult to target ID due to their meandering structure. The phase inversions of the data does make them easy to identify however.
5. high frequency radar systems provide excellent target ID input data

6. surface effects are significant at high frequencies

7. the flow of data to the human operator needs to be minimized in order for the human operator to cope with the data

8. the physical separation between the human operator and the mine detection system is desirable -- both from a safety standpoint and also from an operational endurance standpoint

9. time-frequency filtering applied to the raw data before focusing helps more than spatial filtering applied after focusing

10. a system defined as “isolated, remote, and autonomous” should also be able to fix itself or cope with errors/problems without intervention

References

1. J.E. Mast and E.M. Johansson, “Three-dimensional ground penetrating radar imaging using multi-freauencv diffraction tomography," *Proceedings on Advanced Microwave and Millimeter Wave Detectors,* SPIE Proceedings, Vol. 2275, July 1994.

2. S. D. Nelson, “EM modeling: for GPIR using 3D FDTD modeling; codes.” *Proceedings on Advanced Microwave and Millimeter Wave Detectors,* SPIE Proceedings, Vol. 2275, July 1994.

3. Vivian George, Walcoff and Associates, ``Background Data Collection Test Plan, Fort A. P. Hill, Virginia, Fort Carson, Colorado,” report prepared for *DARPA /Defense Science Office*, Arlington, Virginia, August *30,* 1996.

4. S. G. Azevedo, J. E. Mast, S. D. Nelson, E. T. Rosenbury, “Radar imaging experiments for land-mine detection,” *Lawrence Livermore National Laboratory,* UCRL-JC- 124397, 1996.

5. Humanitarian Deminine Database, *U.S. Army Communications Electronics Command, Night Vision and Electronic Sensors Directorate, Countermine Division, 1997.*

Acknowledgements

This author would like to thank the team participants, Jeffrey E. Mast, Pat Welsh, and Mark Vigars for their outstanding efforts in developing the technology, and preparing for and conducting the field exercises. We would also like to thank Gregory Dallum for his work on the temperature problem with the initial unit, Steve Azevedo for his efforts in management support, and Vivian George of Walcoff & Associates for her efforts in coordinating / directing the site support activities for DARPA.

Appendix I: data acquisition methodology

The LLNL cart based radar system surveyed a number of 1 m x 1 m, 1 m x 2 m, and 1 m x 5 m areas on each of the four test fields. At the Seabee site, the areas selected were based on the Geo-Centers GPR survey results. At the Turkey Creek site, the areas were selected based on site features such as soft soil, hard soil, visual evidence of subsurface clutter, mouse holes, and locations across the site. At the Ft. A. P. Hill sites, the areas were again selected based on a preliminary analysis of the Geo-Centers GPR data. The areas surveyed in the Center Square for each site are provided in Tables l-4. The areas scanned in the yellow and red lanes are as indicated in the DARPA test plan.

The locations that are named starting with a 'Y' are locations from the yellow lane while names starting with an 'R' are locations in the red lane. There were targets associated with each of the locations in the yellow lane except for Y24. The names that start with a 'P' or 'TCC' are located in the Center Square, therefore, no emplaced target was present in those areas.

At each test location, the four comers of the acquisition area that LLNL actually scanned were maked and surveyed by DARPA. A typical configuration is shown in the photo below. The four comers are marked with the orange flags while the yellow flag denotes the center of the coverage area. Those comer locations are tabulated in Tables l-4.

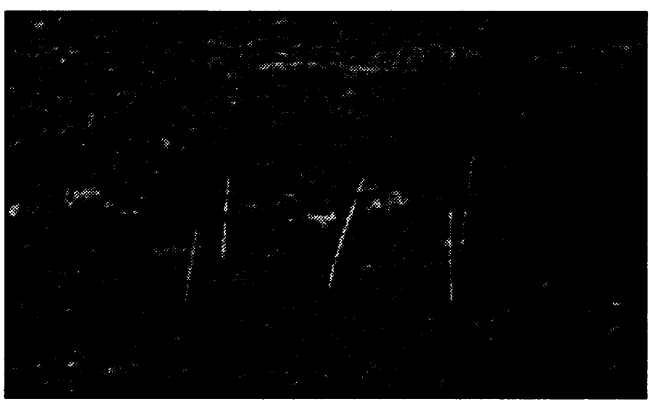

The comer locations were marked and surveyed.

The coordinate notation used in the following tables is *(East, North, Elevation).*

Target	Date	Area (meters)	corner-1 (meters)	corner-2 (meters)	corner-3 (meters)	corner-4 (meters)
Y7	9610.15	1 m × 1 m				
Y8	9610.15	1 m × 1 m				
Y9	9610.15	1 m × 1 m				
Y10 (YT1)	9610.16	1 m × 1 m				
Y11	9610.16	1 m × 1 m				
Y12	9610.16	1 m × 1 m				
Y13	9610.16	1 m × 1 m				
Y16	9610.16	1 m × 1 m				
Y20	9610.16	1 m × 1 m				
Y21	9610.16	1 m × 1 m				
Y24	9610.16	1 m × 1 m				
P14	9610.16	1 m × 5 m	26.12,94.40,100.34	25.97,99.40,100.36	26.98,99.44,100.33	27.13,94.42,100.32
P1	9610.16	1 m × 1 m	32.35,94.27,100.19	32.38,95.26,100.18	33.39,95.28,100.16	33.38,94.28,100.15
P10	9610.16	1 m × 5 m	34.39,83.42,100.20	34.50,88.38,100.16	35.46,88.38,100.09	35.40,83.41,100.16
P5	9610.17	1 m × 1 m	32.52,62.45,100.45	32.51,63.45,100.48	33.53,63.46,100.42	33.53,62.49,100.39
P7	9610.17	1 m × 1 m	29.88,61.81,100.57	29.89,62.81,100.59	30.89,62.80,100.57	30.88,61.81,100.51
P4	9610.17	1 m × 5 m	27.01,33.94,101.06	27.05,38.98,100.95	28.08,38.96,100.91	27.98,33.94,101.01
P3	9610.17	1 m × 5 m	44.44,31.81,100.36	44.58,36.85,100.26	45.57,36.82,100.23	45.45,31.80,100.33
P12	9610.17	1 m × 1 m	41.58,10.29,100.95	41.53,11.29,100.90	42.54,11.33,100.88	42.56,10.32,100.90
P13	9610.17	1 m × 1 m	31.73,20.40,101.03	31.74,21.39,101.00	32.70,21.42,100.96	32.73,20.41,100.98
P2	9610.17	1 m × 5 m	21.63,11.47,101.89	21.58,16.49,101.61	22.57,16.50,101.56	22.63,11.50,101.83
P9	9610.17	1 m × 1 m	60.01,40.78,99.74	60.00,41.73,99.74	61.01,41.69,99.71	61.01,40.77,99.73
P6	9610.17	1 m × 1 m	64.75,68.72,99.50	64.77,69.71,99.48	65.77,69.70,99.48	65.73,68.71,99.49

Table 1. Seabee site survey areas.

The missing entries in the Tables will be provided by DARPA at a later date at their discretion.

Target	Date	Area (meters)	corner-1 (meters)	corner-2 (meters)	corner-3 (meters)	corner-4 (meters)
Y2	9610.18	1 m × 1 m	12.12,3.22,103.03	12.09,4.19,103.09	13.10,4.21,103.06	13.14,3.24,103.00
Y7	9610.18	1 m×1 m	12.09,20.19,103.74	12.07,21.14,103.76	13.06,21.19,103.74	13.08,20.20,103.72
Y8	9610.18	1 m×1 m	12.10,23.16,103.84	12.08,24.15,103.87	13.09,24.17,103.86	13.10,23.19,103.81
Y9	9610.18	1 m×1 m	12.16,26.08,103.95	12.12,27.07,103.99	13.11,27.09,103.96	13.14,26.11,103.93
Y10 (YT1)	9610.18	1 m × 1 m				
Y11	9610.18	1 m × 1 m				
Y12	9610.18	1 m × 1 m				
Y13	9610.18	1 m × 1 m				
Y16	9610.18	1 m × 1 m				
Y20	9610.18	1 m × 1 m				
Y21	9610.18	1 m × 1 m				
Y24	9610.18	1 m × 1 m				
TCC1	9610.18	1 m×5 m	42.40,72.39,104.66	42.42,77.50,104.80	43.41,77.52,104.80	43.40,72.41,104.65
TCC2	9610.19	1 m×5 m	27.11,31.78,103.71	26.98,36.75,103.89	27.97,36.78,103.86	28.11,31.81,103.70
TCC3	9610.19	1 m×5 m	72.90,25.54,103.16	72.91,30.51,103.29	73.91,30.52,103.26	73.92,25.53,103.14
TCC4	9610.19	1 m×5 m	90.34,53.20,103.58	90.35,55.18,103.62	91.35,55.20,103.62	91.35,53.20,103.54
TCC5	9610.19	1 m × 2 m	68.63,71.65,104.30	68.66,73.63,104.35	69.66,73.62,104.34	69.63,71.64,104.29

Table 2. Turkey Creek site survey areas.

Target	Date	Area (meters)	corner-1 (meters)	corner-2 (meters)	corner-3 (meters)	corner-4 (meters)
Y2	9611.18	1 m × 1 m	13.21,4.52,99.75	12.24,4.47,99.79	12.23,3.49,99.77	13.23,3.44,99.76
Y7	9611.18	1 m × 1 m	13.10,21.57,99.66	12.09,21.58,99.67	12.04,20.56,99.68	13.07,20.580,99.67
Y8	9611.18	1 m × 1 m	13.10,24.61,99.60	12.15,24.65,99.64	12.09,23.66,99.64	13.06,23.63,99.65
Y9	9611.18	1 m × 1 m	13.13,27.57,99.55	12.13,27.59,99.57	12.09,26.58,99.56	13.09,26.53,99.55
R5	9611.19	1 m × 1 m	8.64,13.56,99.79	7.63,13.51,99.79	7.54,14.41,99.79	8.57,14.53,99.78
R4	9611.19	1 m × 1 m	8.58,10.57,99.78	7.58,10.49,99.80	7.50,11.55,99.80	8.46,11.61,99.80
Y10 (YT1)	9611.19	1 m × 1 m				
Y11	9611.19	1 m × 1 m				
Y12	9611.19	1 m × 1 m				
Y13	9611.19	1 m × 1 m				
Y16	9611.19	1 m × 1 m				
Y20	9611.19	1 m × 1 m				
Y21	9611.19	1 m × 1 m				
Y24	9611.19	1 m × 1 m				
Y20	9611.21	1 m × 1 m				
Y16	9611.21	1 m × 1 m				
P1	9611.21	1 m × 5 m	18.99,55.02,99.52	19.97,55.06,99.52	19.88,59.95,99.54	19.04,59.99,99.57
P3	9611.21	1 m × 1 m	31.60,63.41,99.30	31.58,62.44,99.29	32.52,62.45,99.20	32.61,63.32,99.31
P2	9611.21	1 m × 5 m	27.90,66.34,99.37	28.91,66.29,99.39	29.19,71.20,99.42	28.24,71.30,99.42
P4	9611.21	1 m × 1 m	41.73,94.21,99.49	41.71,93.29,99.45	42.73,93.30,99.45	42.74,94.18,99.48
P5	9611.21	1 m × 1 m	43.68,39.79,98.94	43.77,38.94,98.82	44.72,38.92,98.88	44.71,39.82,98.91
P8	9611.22	1 m × 5 m	113.57,47.48,99.24	114.55,47.56,99.24	114.73,42.59,99.18	113.69,42.51,99.20
P6	9611.22	1 m × 5 m	147.89,76.92,99.28	146.98,76.95,99.31	146.74,71.88,99.26	147.75,71.90,99.25
P7	9611.22	1 m × 5 m	154.84,0.95,99.44	155.87,0.98,99.43	155.72,6.04,99.37	154.52,6.33,99.57

Table 3. Firing Point 22 site survey areas.

Target	Date	Area (meters)	corner-1 (meters)	corner-2 (meters)	corner-3 (meters)	corner-4 (meters)
Y2	9611.20	1 m × 1 m	13.02,4.58,99.82	12.08,4.59,99.83	12.06,3.56,99.81	12.97,3.54,99.80
Y7	9611.20	1 m×1 m	12.96,21.73,100.09	11.96,21.73,100.09	11.97,20.72,100.09	12.97,20.70,100.08
Y8	9611.20	1 m×1 m	13.06,24.50,100.07	12.05,24.61,100.08	12.01,23.60,100.06	13.00,23.52,100.08
Y9	9611.20	1 m×1 m	13.10,27.50,100.08	12.10,27.51,100.08	12.14,26.55,100.08	13.01,26.50,100.07
Y10 (YT1)	9611.20	1 m × 1 m				
Y11	9611.20	1 m × 1 m				
Y12	9611.20	1 m × 1 m				
Y13	9611.20	1 m × 1 m				
Y16	9611.20	1 m × 1 m				
Y20	9611.20	1 m × 1 m				
Y21	9611.20	1 m × 1 m				
Y24	9611.20	1 m × 1 m				

Table 4. Firing Point 20 site survey areas.

The Center Square area of Firing Point 20 could not be acquired due to the melted snow.

Appendix II: data format

The data formats generated by the LLNL system are a simple set of raw IEEE signed short integer numbers, in LSB byte order, and are typical of the kinds of numbers normally generated by PC based data acquisition systems. Note that LLNL is not using the data format that DARPA requested because each data file would expand to over 320 MB for each 1 m x 1 m data set thus requiring about 90 GB of storage for the entire LLNL data set.

The raw data acquired by LLNL is stored in a series of files maintained by DARPA. The directory structure is laid out to correspond to the acquision date and the specific test point. Thus, a sample of the layout is shown below:

```
ftcarson
          seabee
                         9610.13
                         9610.14
                         9610.15
                         9610.16
                         9610.17
          turkey-creek
                         9610.16
                         9610.17
ftaphill
          fp20
                         9611.20
          fp22
                         9610.18
                         9610.19
                         9610.21
                         9610.22
focused
```

The `ft carson` and `f t aphi 11` data sets consist of two files for each sample area:

1. The raw LSB IEEE 16 bit `signed short int` time domain data (the `. saf` file). This time domain data is stored in 7 x X x Y format with the time axis, 7, being the fastest axis in the data while the scan position, (Y axis), is the slowest axis.

2. The associated header file in ASCII text format (the `. sah` file)

The `. sah` header file is only of intererst in that it contains information about the data file size and axes dimensions. The other information in the header file is for internal use only and provides no meaningful information to those interested in processing the data.

```
%sa_type: 7 (Short)

%sa_size: 512 111 110 1

%sa_byte_order: 0 LSB
```

Where ``type 7'' is `signed short int` data, "byte-order 0 LSB" is least-significant-byte order (little endian), and "size 5 12 111 110 1" is the T x X x Y x S size of the data set. In all of the LLNL data sets: type=7, byte_order=0, and S= 1.

The sequence of the data in the time domain data files uses 7 as the fastest axis and Y as the slowest axis. Thus, the flat data file has the following layout:

```
(t1,x1,y1),(t2,x1,y1),(t3,x1,y1),...(tn,x1,y1),
(t1,x2,y1),(t2,x2,y1),(t3,x2,y1),...(tn,x2,y1),



(t1,xn,y1),(t2,xn,y2),(t3,xn,y1),...(tn,xn,y1),

(t1,x1,y2),(t2,x1,y2),(t3,x1,y2),...(tn,x1,y2),
(t1,x2,y2),(t2,x2,y2),(t3,x2,y2),...(tn,x2,y2),



(t1,xn,y2),(t2,xn,y2),(t3,xn,y2),. .(tn,xn,y2),



.
(t1,xn,ym),(t2,xn,ym),(t3,xn,ym),. .(tn,xn,ym)
```

and may be read using this C code snipet:

```
short int array[ydim][xdim][tdim];
for (y=0; y<ydim; y++){
   for (x=0; x<xdim; x++){
      for (t=0; t<tdim; t++){
         array[y][x][t] = getnextvalue(inputfile);
      }
   }
```

In the cases for the 1 m x 1 m rectangular plots that were taken in the various fields, attempts were made to center the test area over the target of interest. The field measurement accuracy is expected to be a little off because:

- the actual mine burial point and the desired mine burial point are slightly different
- the desired mine burial point was determined by DARPA using a tape measure during LLNL's tests
- the location of the tape measurement spot was marked with a paint spot
- the CART was centered on the paint spot but some wheel slippage could occur
- the four comers of the measurement square were marked with wooden pins
- the wooden pins were replaced by flags
- the coordinates of the flags were measured and are noted in Tables l-4

Table 5 shows the calibration numbers for each data series:

Site	Date	t0 (seconds)	delta_t (seconds)	delta_V (volts)
Seabee, Ft. Carson, CO	9610.14 (R5,Y7,Y8,Y9)	2.430e-10	1.096e-11	2.441e-3
	9610.15 (Y8c,Y9d)	-1.993e-10	1.787e-11	2.441e-3
	9610.16	-3.457e-11	1.770e-11	2.441e-3
	9610.17	-3.064e-11	1.759e-11	2.441e-3
Turkey Creek, Ft. Carson, CO	9610.18 (Y2,Y7,Y8)	-3.504e-10	1.761e-11	1.221e-3
	9610.18 (Y8b,...)	-3.504e-10	1.761e-11	2.441e-3
	9610.19	-6.859e-10	1.838e-11	2.441e-3
Firing Point 20, Ft. A. P. Hill, VA	9611.20	-5.208e-11	1.041e-11	2.441e-3
Firing Point 22, Ft. A. P. Hill, VA	9611.18	7.007e-11	1.001e-11	2.441e-3
	9611.19	8.130e-11	1.016e-11	2.441e-3
	9611.21	-4.881e-10	1.384e-11	2.441e-3
	9611.22	-3.058e-11	1.019e-11	2.441e-3

Table 5. Calibration to absolute units.

where *t0* is the time offset for the first data point in the data, *delta-t* is the time step, and *delta_V* is the voltage step (*V0* = 0). The time is calibrated such that t=0 occurs at the transmit antenna feed. Thus *t0, delta-t,* and *delta_V*, set the absolute calibration of all of the data. The height above the ground was set to 13 cm but varied between 10 cm and 20 cm depending on the localized surface topography.

The following shows a typical time domain waveform from one of the X,Y sample points of an area scan. The first image shows one of the X slices from a scan of an area with the time axis running horizontally in this image and the X running vertically in this image

X axis

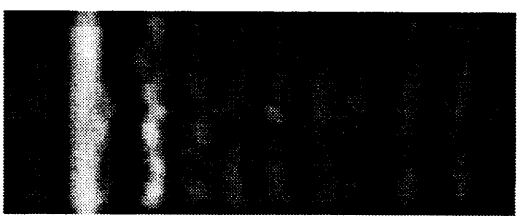

7 axis

while the following graph shows one of the time domain waveforms extracted from this slice

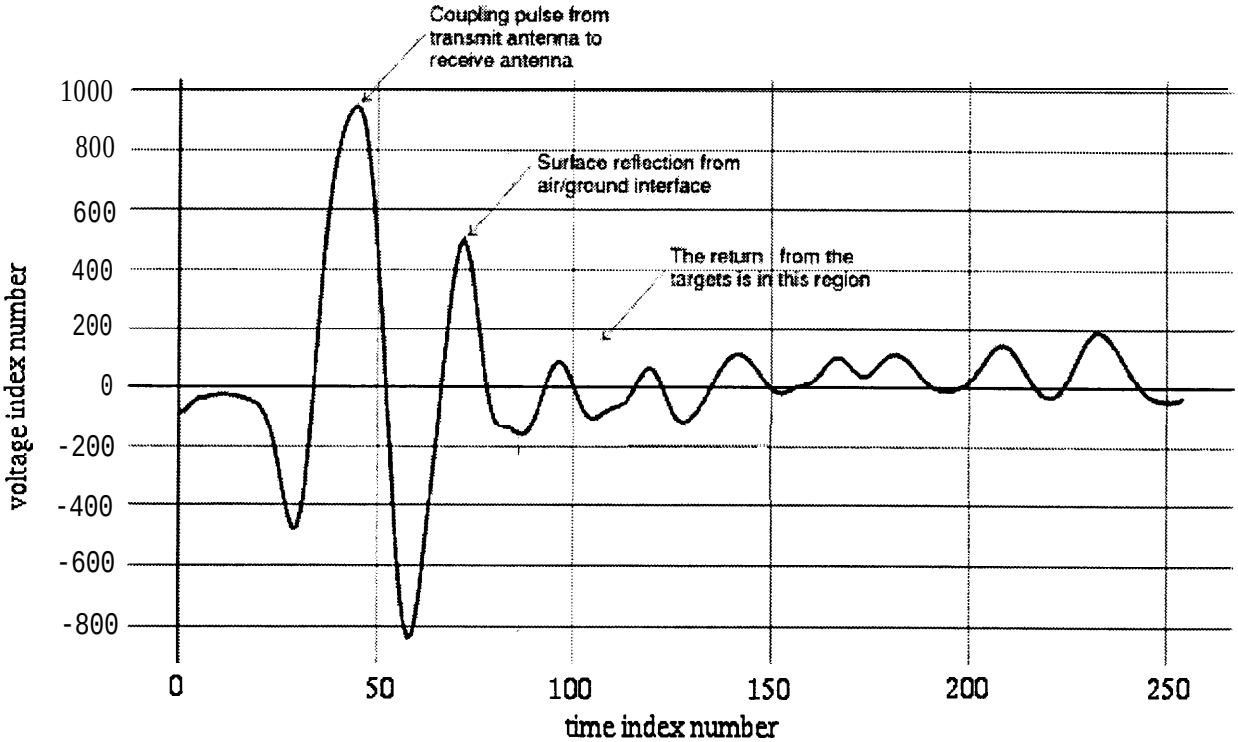

In this case, the vertical axis is the volage index number, *V_index*, and the horizontal axis is the time index number, *t-index.* To get absolute voltage and time, just apply *t0, delta-t,* and *delta_V* from Table 5 using:

$$t = delta\text{-}t * t\text{-}index + t0$$

$$V = delta\_V * V\_index + VO$$

From the color image above, the surface contour of the ground is easly apparent. Do not however assume that a simple peak tracking algorithm will effectively follow the surface return.

Appendix III: focused data

As part of the processing and generation of the focused data sets, a subset of the data sets were converted from LSB IEEE 16 bit `signed short int` to complex data composed of a pair of MSB IEEE 32 bit `float` values via the tomographic reconstructive focusing algorithms [1]. This complex focused data contains information about the magnitude and phase of the RCS return. From there, the data was then converted to an `unsigned char` (byte) rectangular solid on a O-255 scale and stored in X x Y x *Z* format; with X being the fastest axis and *Z* being the slowest axis. In these cases, the file names of the focused images convey the file dimensions. This byte data can easily be loaded into any post processing routine, or volumetric renderer such as BOB or NSD, for display and manipulation purposes. The resolution for each axis of the focused data is:

- X axis: 1 cm
- Y axis: 1 cm
- *Z* axis: 0.25 cm

where 0.25 cm was used for the *Z* axis in order to visually enhance the details in this dimension. Any computer

aided processing of this data should probably recompress the data back down to a 1 cm x 1 cm x 1 cm grid or take the elongation into account. In all cases X was East, Y was North, and Z was the distance into the ground unless otherwise noted.

Anyone desiring to process the LLNL data sets should start with the original raw time domain data. The focused data sets should be used only as a comparison since a significant amount of information was discarded in the generation of the byte representation (notibly, the phase space data is discarded in the complex -> byte conversion).